EUROPEAN ORGANIZATION FOR NUCLEAR RESEARCH

CERN–PPE/93-176

30 September 1993

Production Rate and Decay Lifetime Measurements of B_s^0 mesons at LEP using D_s and ϕ mesons

DELPHI Collaboration

Abstract

The study of the properties of inclusive production of D_s mesons and of events in which a ϕ and a muon are present in the same jet provides two independent measurements of the probability, f_s^w, for a heavy quark to hadronize into a strange B or D meson. The data sample analysed corresponds to 243000 hadronic Z^0 decays recorded in 1991. The combined value of these measurements is $f_s^w = 0.19 \pm 0.06 \pm 0.08$. From the flight distance distributions of D_s and of $(\phi - lepton)$ secondary vertices, with the lepton emitted at high transverse momentum relative to the jet axis, two values are obtained for the B_s^0 meson lifetime. Combining these measurements with a previous result based on the study of $D_s - \mu$ events, the B_s^0 meson lifetime is measured to be : 0.96 ± 0.37 *ps*.

(To be submitted to Zeit. Phys. C.)

P.Abreu[20], W.Adam[7], T.Adye[37], E.Agasi[30], R.Aleksan[39], G.D.Alekseev[14], A.Algeri[13], S.Almehed[23], S.J.Alvsvaag[4], U.Amaldi[7], A.Andreazza[27], P.Antilogus[24], W-D.Apel[15], R.J.Apsimon[37], Y.Arnoud[39], B.Åsman[45], J-E.Augustin[18], A.Augustinus[30], P.Baillon[7], P.Bambade[18], F.Barao[20], R.Barate[12], G.Barbiellini[47], D.Y.Bardin[14], G.J.Barker[34], A.Baroncelli[41], O.Barring[7], J.A.Barrio[25], M.J.Bates[37], M.Battaglia[13], M.Baubillier[22], K-H.Becks[52], M.Begalli[36], P.Beilliere[6], Yu.Belokopytov[43], P.Beltran[9], D.Benedic[8], A.C.Benvenuti[5], M.Berggren[18], D.Bertrand[2], F.Bianchi[46], M.Bigi[46], M.S.Bilenky[14], P.Billoir[22], J.Bjarne[23], D.Bloch[8], J.Blocki[51], S.Blyth[34], V.Bocci[38], P.N.Bogolubov[14], T.Bolognese[39], M.Bonesini[27], W.Bonivento[27], P.S.L.Booth[21], G.Borisov[43], H.Borner[7], C.Bosio[41], B.Bostjancic[44], S.Bosworth[34], O.Botner[48], B.Bouquet[18], C.Bourdarios[18], T.J.V.Bowcock[21], M.Bozzo[11], S.Braibant[2], P.Branchini[41], K.D.Brand[35], R.A.Brenner[7], H.Briand[22], C.Bricman[2], L.Brillault[22], R.C.A.Brown[7], J-M.Brunet[6], A.Budziak[16], L.Bugge[32], T.Buran[32], H.Burmeister[7], A.Buys[7], J.A.M.A.Buytaert[7], M.Caccia[7], M.Calvi[27], A.J.Camacho Rozas[42], R.Campion[21], T.Camporesi[7], V.Canale[38], K.Cankocak[45], F.Cao[2], F.Carena[7], L.Carroll[21], C.Caso[11], M.V.Castillo Gimenez[49], A.Cattai[7], F.R.Cavallo[5], L.Cerrito[38], V.Chabaud[7], A.Chan[1], M.Chapkin[43], Ph.Charpentier[7], L.Chaussard[18], J.Chauveau[22], P.Checchia[35], G.A.Chelkov[14], L.Chevalier[39], P.Chliapnikov[43], V.Chorowicz[22], J.T.M.Chrin[49], V.Cindro[44], P.Collins[34], J.L.Contreras[25], R.Contri[11], E.Cortina[49], G.Cosme[18], F.Couchot[18], H.B.Crawley[1], D.Crennell[37], G.Crosetti[11], J.Cuevas Maestro[33], S.Czellar[13], E.Dahl-Jensen[28], J.Dahm[52], B.Dalmagne[18], M.Dam[32], G.Damgaard[28], E.Daubie[2], A.Daum[15], P.D.Dauncey[34], M.Davenport[7], J.Davies[21], W.Da Silva[22], C.Defoix[6], P.Delpierre[26], N.Demaria[46], A.De Angelis[47], H.De Boeck[2], W.De Boer[15], S.De Brabandere[2], C.De Clercq[2], M.D.M.De Fez Laso[49], C.De La Vaissiere[22], B.De Lotto[47], A.De Min[27], H.Dijkstra[7], L.Di Ciaccio[38], J.Dolbeau[6], M.Donszelmann[7], K.Doroba[51], M.Dracos[7], J.Drees[52], M.Dris[31], Y.Dufour[7], F.Dupont[12], D.Edsall[1], L-O.Eek[48], P.A.-M.Eerola[7], R.Ehret[15], T.Ekelof[48], G.Ekspong[45], A.Elliot Peisert[35], M.Elsing[52], J-P.Engel[8], N.Ershaidat[22], M.Espirito Santo[20], D.Fassouliotis[31], M.Feindt[7], A.Ferrer[49], T.A.Filippas[31], A.Firestone[1], H.Foeth[7], E.Fokitis[31], F.Fontanelli[11], K.A.J.Forbes[21], J-L.Fousset[26], S.Francon[24], B.Franek[37], P.Frenkiel[6], D.C.Fries[15], A.G.Frodesen[4], R.Fruhwirth[50], F.Fulda-Quenzer[18], H.Furstenau[15], J.Fuster[7], D.Gamba[46], C.Garcia[49], J.Garcia[42], C.Gaspar[7], U.Gasparini[35], Ph.Gavillet[7], E.N.Gazis[31], J-P.Gerber[8], P.Giacomelli[7], D.Gillespie[7], R.Gokieli[51], B.Golob[44], V.M.Golovatyuk[14], J.J.Gomez Y Cadenas[7], G.Gopal[37], L.Gorn[1], M.Gorski[51], V.Gracco[11], A.Grant[7], F.Grard[2], E.Graziani[41], G.Grosdidier[18], E.Gross[7], B.Grossetete[22], P.Gunnarsson[45], J.Guy[37], U.Haedinger[15], F.Hahn[52], M.Hahn[45], S.Hahn[52], S.Haider[30], Z.Hajduk[16], A.Hakansson[23], A.Hallgren[48], K.Hamacher[52], G.Hamel De Monchenault[39], W.Hao[30], F.J.Harris[34], V.Hedberg[23], T.Henkes[7], R.Henriques[20], J.J.Hernandez[49], J.A.Hernando[49], P.Herquet[2], H.Herr[7], T.L.Hessing[21], I.Hietanen[13], C.O.Higgins[21], E.Higon[49], H.J.Hilke[7], T.S.Hill[1], S.D.Hodgson[34], T.Hofmokl[51], S-O.Holmgren[45], P.J.Holt[34], D.Holthuizen[30], P.F.Honore[6], M.Houlden[21], J.Hrubec[50], K.Huet[2], K.Hultqvist[45], P.Ioannou[3], P-S.Iversen[4], J.N.Jackson[21], R.Jacobsson[45], P.Jalocha[16], G.Jarlskog[23], P.Jarry[39], B.Jean-Marie[18], E.K.Johansson[45], M.Jonker[7], L.Jonsson[23], P.Juillot[8], G.Kalkanis[3], G.Kalmus[37], F.Kapusta[22], M.Karlsson[45], E.Karvelas[9], S.Katsanevas[3], E.C.Katsoufis[31], R.Keranen[7], B.A.Khomenko[14], N.N.Khovanski[14], B.King[21], N.J.Kjaer[7], H.Klein[7], A.Klovning[4], P.Kluit[30], A.Koch-Mehrin[52], J.H.Koehne[15], B.Koene[30], P.Kokkinias[9], M.Koratzinos[32], K.Korcyl[16], A.V.Korytov[14], V.Kostioukhine[43], C.Kourkoumelis[3], O.Kouznetsov[14], P.H.Kramer[52], M.Krammer[50], C.Kreuter[15], J.Krolikowski[51], I.Kronkvist[23], W.Kucewicz[16], K.Kulka[48], K.Kurvinen[13], C.Lacasta[49], C.Lambropoulos[9], J.W.Lamsa[1], L.Lanceri[47], P.Langefeld[52], V.Lapin[43], I.Last[21], J-P.Laugier[39], R.Lauhakangas[13], G.Leder[50], F.Ledroit[12], R.Leitner[29], Y.Lemoigne[39], J.Lemonne[2], G.Lenzen[52], V.Lepeltier[18], T.Lesiak[16], J.M.Levy[8], E.Lieb[52], D.Liko[50], J.Lindgren[13], R.Lindner[52], I.Lippi[35], B.Loerstad[23], M.Lokajicek[10], J.G.Loken[34], A.Lopez-Fernandez[7], M.A.Lopez Aguera[42], M.Los[30], D.Loukas[9], J.J.Lozano[49], P.Lutz[6], L.Lyons[34], G.Maehlum[32], J.Maillard[6], A.Maio[20], A.Maltezos[9], F.Mandl[50], J.Marco[42], M.Margoni[35], J-C.Marin[7], A.Markou[9], T.Maron[52], S.Marti[49], C.Martinez-Rivero[42], F.Martinez-Vidal[49], F.Matorras[42], C.Matteuzzi[27], G.Matthiae[38], M.Mazzucato[35], M.Mc Cubbin[21], R.Mc Kay[1], R.Mc Nulty[21], J.Medbo[48], G.Meola[11], C.Meroni[27], W.T.Meyer[1], M.Michelotto[35], I.Mikulec[50], L.Mirabito[24], W.A.Mitaroff[50], G.V.Mitselmakher[14], U.Mjoernmark[23], T.Moa[45], R.Moeller[28], K.Moenig[7], M.R.Monge[11], P.Morettini[11], H.Mueller[15], W.J.Murray[37], G.Myatt[34], F.L.Navarria[5], P.Negri[27], S.Nemecek[10], W.Neumann[52], R.Nicolaidou[3], B.S.Nielsen[28], B.Nijjhar[21], V.Nikolaenko[43], P.E.S.Nilsen[4], P.Niss[45], A.Nomerotski[35], V.Obraztsov[43], A.G.Olshevski[14], R.Orava[13], A.Ostankov[43], K.Osterberg[13], A.Ouraou[39], M.Paganoni[27], R.Pain[22], H.Palka[16], Th.D.Papadopoulou[31], L.Pape[7], F.Parodi[11], A.Passeri[41], M.Pegoraro[35], J.Pennanen[13], L.Peralta[20], V.Perevozchikov[43], H.Pernegger[50], M.Pernicka[50], A.Perrotta[5], C.Petridou[47], A.Petrolini[11], G.Piana[11], F.Pierre[39], M.Pimenta[20], S.Plaszczynski[18], O.Podobrin[15], M.E.Pol[17], G.Polok[16], P.Poropat[47], V.Pozdniakov[14], P.Privitera[38], A.Pullia[27], D.Radojicic[34], S.Ragazzi[27], H.Rahmani[31], J.Rames[10], P.N.Ratoff[19], A.L.Read[32], M.Reale[52], P.Rebecchi[7], N.G.Redaelli[27], M.Regler[50], D.Reid[7], P.B.Renton[34], L.K.Resvanis[3], F.Richard[18], J.Richardson[21], J.Ridky[10], G.Rinaudo[46], I.Roditi[17], A.Romero[46], I.Roncagliolo[11], P.Ronchese[35], C.Ronnqvist[13], E.I.Rosenberg[1], E.Rosso[7], T.Rovelli[5], W.Ruckstuhl[30], V.Ruhlmann-Kleider[39], A.Ruiz[42], H.Saarikko[13], Y.Sacquin[39], G.Sajot[12], J.Salt[49], J.Sanchez[25], M.Sannino[11,40], S.Schael[7], H.Schneider[15],

M.A.E.Schyns[52], G.Sciolla[46], F.Scuri[47], A.M.Segar[34], A.Seitz[15], R.Sekulin[37], M.Sessa[47], R.Seufert[15], R.C.Shellard[36], I.Siccama[30], P.Siegrist[39], S.Simonetti[11], F.Simonetto[35], A.N.Sisakian[14], G.Skjevling[32], G.Smadja[39,24], N.Smirnov[43], O.Smirnova[14], G.R.Smith[37], R.Sosnowski[51], D.Souza-Santos[36], T.Spassov[20], E.Spiriti[41], S.Squarcia[11], H.Staeck[52], C.Stanescu[41], S.Stapnes[32], G.Stavropoulos[9], F.Stichelbaut[2], A.Stocchi[18], J.Strauss[50], J.Straver[7], R.Strub[8], B.Stugu[4], M.Szczekowski[7], M.Szeptycka[51], P.Szymanski[51], T.Tabarelli[27], O.Tchikilev[43], G.E.Theodosiou[9], A.Tilquin[26], J.Timmermans[30], V.G.Timofeev[14], L.G.Tkatchev[14], T.Todorov[8], D.Z.Toet[30], O.Toker[13], A.Tomaradze[2], B.Tome[20], E.Torassa[46], L.Tortora[41], D.Treille[7], W.Trischuk[7], G.Tristram[6], C.Troncon[27], A.Tsirou[7], E.N.Tsyganov[14], M-L.Turluer[39], T.Tuuva[13], I.A.Tyapkin[22], M.Tyndel[37], S.Tzamarias[21], B.Ueberschaer[52], S.Ueberschaer[52], O.Ullaland[7], V.Uvarov[43], G.Valenti[5], E.Vallazza[7], J.A.Valls Ferrer[49], C.Vander Velde[2], G.W.Van Apeldoorn[30], P.Van Dam[30], M.Van Der Heijden[30], W.K.Van Doninck[2], J.Van Eldik[30], P.Vaz[7], G.Vegni[27], L.Ventura[35], W.Venus[37], F.Verbeure[2], M.Verlato[35], L.S.Vertogradov[14], D.Vilanova[39], P.Vincent[24], L.Vitale[13], E.Vlasov[43], A.S.Vodopyanov[14], M.Vollmer[52], M.Voutilainen[13], V.Vrba[41], H.Wahlen[52], C.Walck[45], F.Waldner[47], A.Wehr[52], M.Weierstall[52], P.Weilhammer[7], A.M.Wetherell[7], J.H.Wickens[2], M.Wielers[15], G.R.Wilkinson[34], W.S.C.Williams[34], M.Winter[8], M.Witek[16], G.Wormser[18], K.Woschnagg[48], A.Zaitsev[43], A.Zalewska[16], P.Zalewski[18], D.Zavrtanik[44], E.Zevgolatakos[9], N.I.Zimin[14], M.Zito[39], D.Zontar[44], R.Zuberi[34], G.Zumerle[35], J.Zuniga[49]

[1] Ames Laboratory and Department of Physics, Iowa State University, Ames IA 50011, USA
[2] Physics Department, Univ. Instelling Antwerpen, Universiteitsplein 1, B-2610 Wilrijk, Belgium
and IIHE, ULB-VUB, Pleinlaan 2, B-1050 Brussels, Belgium
and Faculté des Sciences, Univ. de l'Etat Mons, Av. Maistriau 19, B-7000 Mons, Belgium
[3] Physics Laboratory, University of Athens, Solonos Str. 104, GR-10680 Athens, Greece
[4] Department of Physics, University of Bergen, Allégaten 55, N-5007 Bergen, Norway
[5] Dipartimento di Fisica, Università di Bologna and INFN, Via Irnerio 46, I-40126 Bologna, Italy
[6] Collège de France, Lab. de Physique Corpusculaire, IN2P3-CNRS, F-75231 Paris Cedex 05, France
[7] CERN, CH-1211 Geneva 23, Switzerland
[8] Centre de Recherche Nucléaire, IN2P3 - CNRS/ULP - BP20, F-67037 Strasbourg Cedex, France
[9] Institute of Nuclear Physics, N.C.S.R. Demokritos, P.O. Box 60228, GR-15310 Athens, Greece
[10] FZU, Inst. of Physics of the C.A.S. High Energy Physics Division, Na Slovance 2, CS-180 40, Praha 8, Czechoslovakia
[11] Dipartimento di Fisica, Università di Genova and INFN, Via Dodecaneso 33, I-16146 Genova, Italy
[12] Institut des Sciences Nucléaires, IN2P3-CNRS, Université de Grenoble 1, F-38026 Grenoble, France
[13] Research Institute for High Energy Physics, SEFT, P.O. Box 9, FIN-00014 University of Helsinki, Finland
[14] Joint Institute for Nuclear Research, Dubna, Head Post Office, P.O. Box 79, 101 000 Moscow, Russian Federation
[15] Institut für Experimentelle Kernphysik, Universität Karlsruhe, Postfach 6980, D-76128 Karlsruhe, Germany
[16] High Energy Physics Laboratory, Institute of Nuclear Physics, Ul. Kawiory 26a, PL-30055 Krakow 30, Poland
[17] Centro Brasileiro de Pesquisas Físicas, rua Xavier Sigaud 150, RJ-22290 Rio de Janeiro, Brazil
[18] Université de Paris-Sud, Lab. de l'Accélérateur Linéaire, IN2P3-CNRS, Bat 200, F-91405 Orsay, France
[19] School of Physics and Materials, University of Lancaster, GB-Lancaster LA1 4YB, UK
[20] LIP, IST, FCUL - Av. Elias Garcia, 14-1°, P-1000 Lisboa Codex, Portugal
[21] Department of Physics, University of Liverpool, P.O. Box 147, GB-Liverpool L69 3BX, UK
[22] LPNHE, IN2P3-CNRS, Universités Paris VI et VII, Tour 33 (RdC), 4 place Jussieu, F-75252 Paris Cedex 05, France
[23] Department of Physics, University of Lund, Sölvegatan 14, S-22363 Lund, Sweden
[24] Université Claude Bernard de Lyon, IPNL, IN2P3-CNRS, F-69622 Villeurbanne Cedex, France
[25] Universidad Complutense, Avda. Complutense s/n, E-28040 Madrid, Spain
[26] Univ. d'Aix - Marseille II - CPP, IN2P3-CNRS, F-13288 Marseille Cedex 09, France
[27] Dipartimento di Fisica, Università di Milano and INFN, Via Celoria 16, I-20133 Milan, Italy
[28] Niels Bohr Institute, Blegdamsvej 17, DK-2100 Copenhagen 0, Denmark
[29] NC, Nuclear Centre of MFF, Charles University, Areal MFF, V Holesovickach 2, CS-180 00, Praha 8, Czechoslovakia
[30] NIKHEF-H, Postbus 41882, NL-1009 DB Amsterdam, The Netherlands
[31] National Technical University, Physics Department, Zografou Campus, GR-15773 Athens, Greece
[32] Physics Department, University of Oslo, Blindern, N-1000 Oslo 3, Norway
[33] Dpto. Fisica, Univ. Oviedo, C/P.Jimenez Casas, S/N-33006 Oviedo, Spain
[34] Department of Physics, University of Oxford, Keble Road, Oxford OX1 3RH, UK
[35] Dipartimento di Fisica, Università di Padova and INFN, Via Marzolo 8, I-35131 Padua, Italy
[36] Depto. de Fisica, Pontificia Univ. Católica, C.P. 38071 RJ-22453 Rio de Janeiro, Brazil
[37] Rutherford Appleton Laboratory, Chilton, GB - Didcot OX11 OQX, UK
[38] Dipartimento di Fisica, Università di Roma II and INFN, Tor Vergata, I-00173 Rome, Italy
[39] Centre d'Etude de Saclay, DSM/DAPNIA, F-91191 Gif-sur-Yvette Cedex, France
[40] Dipartimento di Fisica-Università di Salerno, I-84100 Salerno, Italy
[41] Istituto Superiore di Sanità, Ist. Naz. di Fisica Nucl. (INFN), Viale Regina Elena 299, I-00161 Rome, Italy
[42] C.E.A.F.M., C.S.I.C. - Univ. Cantabria, Avda. los Castros, S/N-39006 Santander, Spain
[43] Inst. for High Energy Physics, Serpukov P.O. Box 35, Protvino, (Moscow Region), Russian Federation
[44] J. Stefan Institute and Department of Physics, University of Ljubljana, Jamova 39, SI-61000 Ljubljana, Slovenia
[45] Fysikum, Stockholm University, Box 6730, S-113 85 Stockholm, Sweden
[46] Dipartimento di Fisica Sperimentale, Università di Torino and INFN, Via P. Giuria 1, I-10125 Turin, Italy
[47] Dipartimento di Fisica, Università di Trieste and INFN, Via A. Valerio 2, I-34127 Trieste, Italy
and Istituto di Fisica, Università di Udine, I-33100 Udine, Italy
[48] Department of Radiation Sciences, University of Uppsala, P.O. Box 535, S-751 21 Uppsala, Sweden
[49] IFIC, Valencia-CSIC, and D.F.A.M.N., U. de Valencia, Avda. Dr. Moliner 50, E-46100 Burjassot (Valencia), Spain
[50] Institut für Hochenergiephysik, Österr. Akad. d. Wissensch., Nikolsdorfergasse 18, A-1050 Vienna, Austria
[51] Inst. Nuclear Studies and University of Warsaw, Ul. Hoza 69, PL-00681 Warsaw, Poland
[52] Fachbereich Physik, University of Wuppertal, Postfach 100 127, D-5600 Wuppertal 1, Germany

1 Introduction

In this article a study of strange B meson production in 243,000 hadronic Z^0 decays recorded in the DELPHI detector in 1991 is reported. Using two independent inclusive channels, the B_s^0 production rate and the decay lifetime have been measured. The study of $B_s^0/\bar{B}_s^0$ oscillations, providing important constraints on the C.K.M. matrix elements and leading to a measurement of the phase responsible for CP violation, will become possible when the available statistics are considerably greater than at present.

B_s^0 mesons are expected to be produced at a rate an order of magnitude smaller than non-strange B mesons; thus decay channels which allow strong rejection against non-strange B-hadrons have to be used. In a recent publication [1] evidence has been given for the production of B_s^0 mesons at LEP from the observation of seven events in which a muon and a D_s meson were present in the same jet. The muon was required to have large transverse momentum (p_t^l) relative to the jet axis, and, as a consequence, the sample was enriched in direct B-hadron semi-leptonic decays. The D_s meson, exclusively reconstructed through the $\phi\pi$ or $\bar{K}^{\star 0}K$ decay modes, signalled the B_s^0.

To increase statistics, two more inclusive decay channels have been used for the present analysis. Since the presence of a D_s meson provides an enriched B_s^0 sample, the first consists of events containing a D_s meson decaying to $\phi\pi$. The second sample contains events with a high p_t^l lepton accompanied by a ϕ meson in the same jet.

In section 2, a description of the components of the DELPHI detector which are used in this analysis is given. The inclusive production of D_s meson and of $(\phi - lepton)$ events are treated in section 3 and 4 respectively .

Since these studies are based on samples of events rich in strange D or B hadrons, the measured rate of the selected events is used to evaluate the probability, f_s^w, that a weakly decaying strange heavy meson is produced during the hadronization process of a c or a b quark. Throughout this paper this parameter is assumed to have the same value for the two flavours of heavy quarks. It differs from the usual probability, f_s, that a heavy quark hadronizes with a strange antiquark because of the possible production of $D_s^{\star\star}$ or $B_s^{0\star\star}$ states that could decay into non-strange D or B mesons (non-strange $D^{\star\star}$ or $B^{\star\star}$ states can conversely decay into D_s or B_s mesons). Also, f_s^w is more directly related to the measurements and is independent of the modelling of the hadronization mechanism. Similarly, f_{baryon}^w is the probability that a weakly decaying heavy baryon be produced by the hadronization of a heavy flavour quark.

The two selected samples of events have also been used to measure the B_s^0 meson lifetime.

2 The detector

The components of the DELPHI detector which play an important role in the present analysis are described here. A complete description of the DELPHI apparatus is given in [2].

The muon identification relies mainly on the muon detector, a set of drift chambers (each with 2 layers) providing three dimensional information. In the barrel part three sets of chambers (MUB) cover polar angles between 52° and 128°, with the first located inside the magnet return yoke, the second set just outside the yoke, and the third set further out having a small overlap with the others. The two sets of forward muon chambers (MUF) cover polar angles between 9° and 43° and between 137° and 171°. In each arm the first set is located inside the yoke and the second outside.

The central tracking system, comprising the inner detector (ID), the time projection chamber (TPC) and the outer detector (OD), measures the charged particle tracks at polar angles between 30° and 150° with a resolution of $\sigma(p)/p \simeq 0.0013 \times p$, ($p$ in GeV/c). The TPC, the main tracking device, is a cylinder of 30 cm inner radius, 122 cm outer radius and length 2.7 m. For the polar angles between 39° and 141° it provides up to 16 space points along the charged particle trajectory. The energy loss (dE/dX) for each charged particle is measured by the 192 TPC sense wires as the truncated mean of the smallest 80 % of the wire signals. Using $Z^0 \to \mu^+\mu^-$ events, the dE/dX resolution has been measured to be 5.5 %. For particles in hadronic jets the resolution is 7.5 %, and for 25 % of the particles the dE/dX is not measured due to the presence of another charged particle within the two-track resolution distance in z of the TPC.

The Microvertex detector (VD) [3] is made of three concentric shells of silicon-strip detectors at radii of 6.3, 9 and 11 cm covering the central region of the DELPHI apparatus at polar angles between 27° and 153°. The shells surround the beam pipe, a beryllium cylinder 1.45 mm thick with a 5.3 cm inner radius. Each shell consists of 24 modules with about 10 % overlap in azimuth between the modules. Each module holds 4 detectors with strips parallel to the beam direction. The silicon detectors are 300 μm thick and have a diode pitch of 25 μm. The read-out strips (50 μm pitch) are AC-coupled and give a 5 μm intrinsic precision on the coordinates of the charged particle tracks, transverse to the beam direction. After a careful procedure of relative alignment of each single detector, an overall precision of 8 μm has been achieved. Using the combined information from OD, TPC, ID and VD a resolution of 3.5 % on $\sigma(p)/p$ has been obtained for 45 GeV/c muons.

3 Inclusive D_s meson production

3.1 D_s production in Z^0 decays

The decay of a B meson usually yields a charmed hadron. The simplest way to represent this process is by the spectator quark model where the b to c transition occurs via the emission of a virtual W which couples to a lepton anti-neutrino or a $\bar{u}d$ pair. The resultant c quark recombines with the spectator antiquark to form a D meson. The corresponding diagram (figure 1-a) shows a B_s^0 meson decaying to a D_s with either a charged lepton anti-neutrino pair or light meson(s). Other B-meson decay diagrams also contribute and have been included in the version of the JETSET 7.3 generator [4] program presently used in DELPHI. The branching ratios of the B decays have been tuned to reproduce the measured inclusive decay properties of B^0 and B^+ mesons. According to this simulation program, which uses the same type of decay mechanisms for all B hadrons, the inclusive branching fraction $Br(B_s^0 \to D_s X)$ is 70%, which agrees with a theoretical calculation giving $Br(B_s^0 \to D_s X) = 86\ ^{+8}_{-13}\%$ [5]. The latter value has been used in this analysis.

There are, however, other sources of D_s mesons in Z^0 decays : the hadronization of charm quarks coming directly from the Z^0 (figure 1-b) and the decays of non-strange B's which produce a D_s mainly in the quasi two-body process $B \to D^{(*)} D_s^{(*)}$ (figure 1-c). The purity of B_s^0 in a D_s sample will therefore depend both on the relative strength of these different sources and on the experimental selection procedure.

Initial estimates of the branching ratios for the processes illustrated in figure 1 have been made by assuming that

- the couplings of the Z^0 to $c\bar{c}$ and $b\bar{b}$ quarks pairs agree with the Standard Model expectation ($\frac{\Gamma_{Z^0\to c\bar{c}}}{\Gamma_{Z^0\to Hadrons}} = 0.171$ and $\frac{\Gamma_{Z^0\to b\bar{b}}}{\Gamma_{Z^0\to Hadrons}} = 0.217$),
- the hadronization of c and b quarks into heavy hadrons is given by the JETSET 7.3 generator program ($f_s^w = 0.12$, $f_{baryon}^w = 0.08$, $Prob(b \to B_{u,d}) = 0.8$) and
- the production of D_s mesons in B^- or B_d^0 decays is the same as the one measured in Υ(4S) decays ($Br(B_{u,d} \to D_s X) = 10.0 \pm 2.0(stat) \pm 4.0(syst)$ % [6]),

obtaining :

$$Br(Z^0 \to B_s^0 \to D_s X) = \frac{\Gamma_{Z^0\to b\bar{b}}}{\Gamma_{Z^0\to Hadrons}} \times 2 \times f_s^w \times Br(B_s^0 \to D_s X) = 4.5\ \%$$

$$Br(Z^0 \to c\bar{c} \to D_s X) = \frac{\Gamma_{Z^0\to c\bar{c}}}{\Gamma_{Z^0\to Hadrons}} \times 2 \times f_s^w = 4.1\ \%$$

$$Br(Z^0 \to B_{u,d} \to D_s X) = \frac{\Gamma_{Z^0\to b\bar{b}}}{\Gamma_{Z^0\to Hadrons}} \times 2 \times (1 - f_s^w - f_{baryon}^w) \times Br(B_{u,d} \to D_s X) = 3.5\ \%$$

Hereafter D_s mesons produced in the process of figure 1-b will be referred to as direct D_s and those coming from the processes of figures 1-a and 1-c as cascade D_s.

Using the kinematical cuts described below for selecting events with a D_s meson, the contribution from direct D_s is suppressed and a sample of events enriched in B_s^0 mesons is obtained.

3.2 Reconstruction of D_s mesons

Events containing D_s mesons are selected by the decay of a D_s to $\phi\pi$ ($Br(D_s \to \phi\pi) = 3.0 \pm 1.0\%$ [6]) with the ϕ decaying to a K^+K^- system. The narrow width (4.4 MeV) of the ϕ meson and its position (1020 MeV), close to threshold, in the K^+K^- mass distribution ensure a low combinatorial background. The spatial and the momentum resolutions of charged particles reconstructed in the central tracking detectors are considerably improved when the reconstructed trajectory can be associated to points measured in the vertex detector. Only particles with momentum greater than 1 GeV (0.5 GeV for the candidate pion) with at least two associated hits in the VD and having an impact parameter with respect to the fitted primary vertex less than 2 mm in the transverse plane are used in the analysis.

The invariant mass of pairs of oppositely charged particles is computed with each particle assigned the kaon mass and with the requirement that the ionisation in the TPC for each track be either unmeasured or lower than the one expected for a pion of the same momentum.

For illustration purposes in figure 2 the K^+K^- mass spectrum is shown for particles passing a stronger cut on the ionization, namely requiring that the ionization be measured and smaller than 90 % of that expected for a pion of the same momentum. The ϕ peak is observed at 1020.2 ± 0.5 MeV and has a width of 4.6 ± 0.5 MeV. This mass resolution is consistent with the expected value from the Monte Carlo simulation.

Secondary vertices are reconstructed for each pair of charged particles with a (K^+K^-) mass within $\pm$ 12 MeV of the nominal ϕ mass with a third charged particle (assumed to be a pion) in the same jet. The 3-prong combination is retained as a D_s candidate if

- the vertex χ^2 probability is greater than 1 %,

- the distance, projected in the plane perpendicular to the beam, from the primary interaction point is larger than the experimental error on the flight path (typically 300 μm),
- the angle ψ between the kaon and the pion in the ϕ rest frame satisfies the condition $|\cos(\psi)| > 0.4$,
- the angle θ^*, defined as the angle between the ϕ direction in the D_s rest frame and the D_s line of flight in the laboratory, satisfies the condition $\cos(\theta^*) > -0.8$ and
- the fraction of the beam energy taken by a D_s meson ($x = E_{D_s}/E_{beam}$) is smaller than 0.5 (this reduces the direct D_s contribution).

The resulting $\phi\pi$ invariant mass distribution is shown in figure 3. A clear signal, centered at 1962 $\pm$ 2 MeV, containing 58 $\pm$ 12 events can be seen. This peak lies 7 MeV below the nominal D_s mass; a similar displacement has been observed by this collaboration on other reconstructed charm signals such as $D^0 \rightarrow K^-\pi^+$ [7] and has been attributed to residual distortions in the relative alignment of individual tracking detectors.

The $\cos(\psi)$ distribution, before the cut on this variable, has been studied to verify that the signal behaves as expected for a pseudoscalar particle decaying into a vector plus a pseudoscalar particle. The $|\cos(\psi)|$ distribution (see figure 4-a) after background subtraction is found to be consistent with the expected $\cos^2(\psi)$ behaviour. The tight cut on the K^+K^- mass has the effect of strongly suppressing contributions to the signal from kinematical reflections of other charmed mesons.

3.3 Measurement of f_s^w from inclusive D_s meson production

The efficiencies of the selection criteria are not the same for each of the processes contributing to the observed D_s meson sample. The respective contributions from the processes of figure 1-a, 1-b and 1-c are different from the production rates given in section 3.1 . The cuts applied on the measured decay length and on the beam energy fraction taken by the D_s meson reduce the contribution from direct D_s. These efficiencies have been determined from the Monte Carlo samples to be $11.6 \pm 0.6(stat)$ % and $4.7 \pm 0.8(stat)$ % for the cascade and the direct D_s meson samples, respectively, not including the branching fraction of the ϕ meson into K^+K^-.

The residual contribution of direct D_s has been studied as a function of the transverse momentum of the D_s measured with respect to the jet axis. The latter is computed using charged particles including the decay products of the D_s. This distribution, shown in figure 4-b, has been fitted to a linear combination of the distributions for direct and cascade D_s obtained from Monte Carlo simulation. An upper limit of 9.3 events is obtained for the contribution of the direct D_s component using its fitted value increased by 1 standard deviation. This component corresponds then to less than 16 % of the total number of candidates.

A consistency check of the enrichment of the sample in cascade D_s is obtained from the distribution of the apparent lifetime of the D_s defined as $\tau_{app} = L \ / \ (\gamma\beta c \sin(\theta))$ where L is the distance, in the transverse plane, between the primary vertex and the D_s decay vertex. Selecting events with a transverse momentum larger than 0.5 GeV, the mean apparent D_s lifetime has been measured to be 1.3 $\pm$ 0.4 ps. This value can be compared to the corresponding expectation from the Monte Carlo simulation of 1.5 ps for cascade and 0.6 ps for direct D_s meson production (this latter value is not equal to the true D_s lifetime because of the cut on the flight path previously described). This argument is valid if the B_s^0 lifetime is not too different from the value of 1.2 ps used in

the Monte Carlo simulation ; this assumption is in agreement with the result obtained in this article (see section 5).

The contribution of direct D_s has been computed from the production rate measured by ARGUS and CLEO [8,9] below the threshold for B meson production and from the inclusive cross-section $\sigma(e^+e^- \to c\bar{c})$ measured at the same energy, resulting in $Prob(c \to D_s)Br(D_s \to \phi\pi) = 0.300 \pm 0.045\%$ [9]. Assuming that this probability does not depend on the centre of mass energy, this corresponds to 5.8 ± 1.3 reconstructed events which have been subtracted from the observed sample. Correcting the number of reconstructed D_s mesons for the overall acceptance and efficiency and assuming the Standard Model value $\Gamma(Z^0 \to b\bar{b})/\Gamma(Z^0 \to hadrons) = 0.217$, the inclusive fraction of B decays to D_s mesons, subsequently decaying into $\phi\pi$, at LEP energies is :

$$B_1 = Br(b \to D_s X)Br(D_s \to \phi\pi) = (8.5 \pm 1.9(stat) \pm 1.0(syst)) \times 10^{-3}$$

The same quantity has been measured at the $\Upsilon(4S)$, where no B_s^0 mesons are produced, by ARGUS and CLEO collaborations [10] giving a combined value of :

$$B_2 = Br(b \to D_s X))|_{\Upsilon(4S)}Br(D_s \to \phi\pi) = (2.99 \pm 0.35) \times 10^{-3}$$

This clearly implies an excess, E_s, of inclusive D_s production in B decays at LEP. The measured excess can be attributed to the production of D_s mesons in B_s^0 decays and calculated from $E_s = B_1 - (1 - f_s^w)B_2$. Using, conservatively, $(1 - f_s^w) = 0.8 \pm 0.2$ this excess is found to be

$$E_s = Br(b \to B_s^0 \to D_s X)Br(D_s \to \phi\pi) = (6.1 \pm 1.9(stat) \pm 1.2(syst)) \times 10^{-3}$$

This measurement confirms the production of B_s^0 mesons reported earlier in the study of D_s production in association with a charged lepton [1].

Alternatively the measurement of B_1 and B_2 together with the $Br(D_s \to \phi\pi) = 3 \pm 1\%$ and $Br(B_s^0 \to D_s X) = 86\ ^{+8}_{-13}\%$ can be used to evaluate f_s^w from

$$B_1 = f_s^w Br(B_s^0 \to D_s X)Br(D_s \to \phi\pi) + (1 - f_s^w)B_2$$

In this way the probability of a b quark fragmenting into a B_s^0 meson is determined to be

$$f_s^w = 0.24 \pm 0.08(stat)\ ^{+0.15}_{-0.09}(syst)$$

The sources of the systematic error and their contributions are listed in Table 1.

The systematic uncertainty on the selection efficiency takes into account both the difference between the Monte-Carlo simulation and the actual performance of the DELPHI detector and the dependence of this efficiency on the B_s^0 meson lifetime [11]. The latter effect provides the dominant contribution giving a 5 % change in the selection efficiency for a 20 % variation around the central value of 1.2 ps for the B_s^0 meson lifetime used in the Monte Carlo.

3.4 A measurement of the B_s^0 meson lifetime

For a lifetime measurement of B_s^0, the selected sample of events has to have a high signal to background ratio. To achieve this the selection criteria described in section 3.2 have been tightened, in particular those based on the TPC particle identification because they are not correlated with the variables used in this measurement. It was required that

- the ionisation information be present for both kaon candidates and be compatible, at the level of one standard deviation, with the kaon hypothesis,

Table 1: Systematic errors on f_s^w determination

Systematic source	Parameter range	Absolute variation on f_s^w
$Br(D_s \to \phi\pi)$	3 ± 1 %	$^{-0.07}_{+0.14}$
$Br(B_s^0 \to D_s X)$	$86\ ^{+8}_{-13}$ %	$^{-0.03}_{+0.05}$
$Br(b \to D_s X)\vert_{\Upsilon(4S)} Br(D_s \to \phi\pi)$	$(2.99 \pm 0.35) \times 10^{-3}$	∓ 0.01
Selection efficiency	11.7 ± 1.3 %	∓ 0.04

- the K^+K^- mass be within 8 MeV of the ϕ mass (1020 MeV),
- the transverse momentum of the D_s ($p_t^{D_s}$) be greater than 0.5 GeV.

The residual component due to direct D_s production was reduced to 0.6 ± 0.4 events by the $p_t^{D_s}$ cut. The resulting $\phi\pi$ mass spectrum is shown in the inset of fig.5. In the mass interval between 1940 and 1970 MeV/c^2, 17 events pass these cuts of which 2.8 ± 0.8 can be attributed to the combinatorial background.

For these events a B meson proper lifetime was defined as:

$$t_B = \frac{L/(c\sin(\theta_{D_s})) - \gamma_{D_s}\beta_{D_s}\tau_{D_s}}{\gamma_B\beta_B}$$

where L is the distance between the primary vertex and the D_s decay vertex in the transverse plane. γ_B has been estimated using a parametrisation of the relation between γ_B and the D_s energy. The form $1/\gamma = a/(E_D + b) + c$ with $a = 0.314 \pm 0.006\ GeV$, $b = -4.03 \pm 0.07\ GeV$ and $c = 0.1313 \pm 0.0004$, determined from Monte Carlo simulation, has been used. After this rescaling, the B_s^0 energy resolution is found to be 21 %.

A maximum likelihood fit has been performed on the proper decay time distribution shown in fig. 5. The fitting function was made up of a superposition of two distributions:

- the distribution for B_s^0 events, determined from Monte Carlo, taking into account the experimental resolution on the flight distance, the smearing of the estimated γ_B factor for B_s^0 and the effect of the cut on the flight distance and
- the distribution for background, as measured from two control regions either side of the signal in the mass distribution.

The B lifetime, the only parameter of the fit, was determined to be

$$\tau(B \to D_s X) = 0.94\ ^{+0.35}_{-0.22}(stat) \pm 0.15(syst)\quad ps$$

The dominant contributions to the systematic error come from the background parametrisation and from the uncertainty on the parameters of the relation between γ_B and the D_s energy.

Using the combined measurement of f_s^w (0.19 ± 0.10 - see section 5) presented in this article the purity in B_s^0 meson of this sample is estimated to be $71 \pm 8 \pm 6\%$. Using the average value for the B lifetime [12] a determination of the B_s^0 lifetime was obtained :

$$\tau(B_s^0) = 0.75\ ^{+0.49}_{-0.33}\,(stat) \pm 0.22\ (syst)\, ps$$

4 Inclusive associated production of ϕ meson and lepton

A second sample of events rich in B_s^0 mesons, independent of the sample just described, has been obtained by selecting events containing a high p_t^l lepton accompanied by a ϕ meson in the same jet. The ϕ meson is more likely to be a decay product of D_s than of non-strange charm hadrons because of the presence of a strange valence quark in the D_s. The inclusive production rate for ϕ from decays of D^+ and D^0 due to Cabibbo suppressed transitions and also due to W-exchange diagrams for the D^0, or from final-state interactions has not been measured. Nevertheless, from the measured exclusive decay channels, it has been shown [13] that the inclusive rate of ϕ mesons from D^0, D^+ and D_s meson production can be inferred with reasonable accuracy. Also, it has been shown, in section 3, that the probability that a D_s meson is produced in a B_s^0 meson decay is an order of magnitude larger than in non-strange B meson decays.

A sample of events with a ϕ meson is thus likely to contain a mixture of b and c quark events (direct and cascade D_s events of section 3). The additional requirement of an identified charged lepton in the same jet reduces the contribution of light quarks to the production of ϕ mesons.

Since prompt leptons from B meson decays are emitted at larger transverse momenta than in direct charm or cascade B meson decays, selection of events with a ϕ meson and a charged lepton emitted at large p_t^l should provide a substantially enriched sample of B_s^0 decays.

4.1 Selection of ϕ meson-lepton events

To measure the B_s^0 production rate from $\phi - lepton$ events only muons are used. Details on muon identification are given in [14]. The identified muon is required to have associated hits in at least two layers of the VD and a measured momentum greater than 2 GeV/c.

In each event with an identified muon all other charged particle tracks with an impact parameter less than 2 mm are used to reconstruct the primary vertex using the known position of the beam spot as a constraint. If the primary vertex fit has a χ^2-probability less than 10^{-3}, an iterative procedure is applied removing, at each iteration, the track contributing most to the χ^2. In a Monte Carlo generated $b\overline{b}$ sample, this procedure is found to reconstruct vertices with an accuracy of 80 μm in the horizontal direction, where the beam spot has the larger spread, and 40 μm vertically.

Charged particles are then separated in two hemispheres by the plane orthogonal to the event thrust axis and containing the primary vertex. It has also been required that the two kaons and the lepton form a vertex with a χ^2-probability greater than 10^{-3}. The invariant mass of pairs of oppositely charged particles, assigned the kaon mass, having momentum greater than 2.5 GeV/c and in the same hemisphere as the identified muon is shown in figure 6-a. A signal of 51 ± 11 events is observed centered at the expected ϕ mass. Restricting the sample to events with the muon having transverse momentum greater than 1 GeV/c (to the jet axis determined without including the muon) the observed ϕ signal is 22 ± 6 as shown in figure 6-b. The cut on the transverse momentum of the μ improves the signal to noise ratio by a factor 2.

4.2 Measurement of f_s^w from ϕ meson-lepton correlations

In order to extract f_s^w from the data, the different sources of signal and background have been examined. Three main processes contributing to the selected events are listed below in decreasing value of the mean transverse momentum of the muon with their probabilities per hadronic Z^0 decay. The different probabilities for a given process I are noted P_I^x where the letter x refers to a subprocess which depends mainly on the strangeness content of the decaying heavy hadron. These different subprocess are displayed in Fig. 7.

- process 1 : the muon is produced in the direct semileptonic decay of a B meson. Two processes contribute - from strange and non-strange initial B mesons (figure 7-a) :

$$P_1^a = 2 \times (\frac{\Gamma_{Z^0 \to b\overline{b}}}{\Gamma_{Z^0 \to Hadrons}}) \times f_s^w \times (Br(B_s^0 \to D_s \mu X)^* \times Br(D_s \to \phi X)^* + Br(B_s^0 \to D_{ns} \mu X)^* \times Br(D_{ns} \to \phi X)^*)$$

  where D_{ns} means non-strange D mesons, and (figure 7-b)

$$P_1^b = 2 \times (\frac{\Gamma_{Z^0 \to b\overline{b}}}{\Gamma_{Z^0 \to Hadrons}}) \times (1 - f_s^w - f_{baryon}^{w*}) \times (Br(B \to D^0 \mu X) \times Br(D^0 \to \phi X)^* + Br(B \to D^+ \mu X) \times Br(D^+ \to \phi X)^*)$$

  Non strange B meson semileptonic decay to D_s is highly suppressed since it requires a cascade $B \to D^{**} \to D_s$ and hence has not been included.
- process 2 : both the muon and the ϕ come from a D meson produced in the cascade decay of a B meson. There are three main sub-classes :
  1. the initial B meson is not strange ; the ϕ and the μ are produced through decays of two different D hadrons (figure 7-c) :

$$P_2^c = 2 \times (\frac{\Gamma_{Z^0 \to b\overline{b}}}{\Gamma_{Z^0 \to Hadrons}}) \times (1 - f_s^w - f_{baryon}^{w*}) \times Br(B \to D_s D X) \times (Br(D \to \mu X) \times Br(D_s \to \phi X)^* + Br(D_s \to \mu X) \times Br(D \to \phi X)^*)$$

  2. the initial B meson is a B_s^0 ; both the ϕ and the μ are produced through the decay of a D_s meson (figure 7-d) :

$$P_2^d = 2 \times (\frac{\Gamma_{Z^0 \to b\overline{b}}}{\Gamma_{Z^0 \to Hadrons}}) \times f_s^w \times Br(B_s^0 \to D_s X)^* \times Br(D_s \to \phi \mu \nu)$$

  3. the initial B meson is not strange ; both the ϕ and the μ are produced through the decay of a D_s meson (figure 7-e) :

$$P_2^e = 2 \times (\frac{\Gamma_{Z^0 \to b\overline{b}}}{\Gamma_{Z^0 \to Hadrons}}) \times (1 - f_s^w - f_{baryon}^{w*}) \times Br(B \to D_s X) \times Br(D_s \to \phi \mu \nu)$$

- process 3 : the muon comes from the semileptonic decay of a D meson produced in $Z^0 \to c\overline{c}$ events (figure 7-f). Only D_s semileptonic decays are expected to contribute to this process :

$$P_3^f = 2 \times (\frac{\Gamma_{Z^0 \to c\overline{c}}}{\Gamma_{Z^0 \to Hadrons}}) \times f_s^w \times Br(D_s \to \phi \mu \nu)$$

In these expressions it has been assumed that B baryons were not contributing to $\phi - l$ events ; this assumption gives a negligible contribution to the overall systematic uncertainty attached to the measurement of f_s^w.

In the above expressions, quantities marked by a (*) have not been directly measured up to now and their possible ranges of variation are studied below.

The inclusive branching fractions of the D^0, D^+ and ${D_s}^+$ mesons into a ϕ meson have been considered in [13], and the following values are found to be most likely

$$Br(D_s \to \phi X) \;=\; (4.8 \pm 0.5) \times Br(D_s \to \phi\pi^+)$$

$$Br(D^0 \to \phi X) \;=\; (1.8 \pm 0.3)\ \%$$

$$Br(D^+ \to \phi X) \;=\; (1.7 \pm 0.3)\ \%$$

As indicated in section 3.1, the inclusive branching fraction $B_s^0 \to D_s\ X$ is assumed to be $86^{+8}_{-13}\%$.

The probability of a b quark fragmenting to a B baryon, f^{w*}_{baryon}, is assumed to lie within 5 and 15 % (set to 8 % in JETSET 7.3).

The expected fractions of strange and non-strange D mesons produced in the semileptonic decays of B_s^0 mesons have been inferred from the D^{**} production rate measured in non-strange B decays [15]. For the transitions $B_s^0 \to D_s l\nu$ and $B_s^0 \to D_s^* l\nu$, a D_s meson is always produced in the final state, whereas in case of $B_s^0 \to D_s^{**} l\nu$ or $B_s^0 \to DK(n\pi)l\nu$ decays, the produced charmed meson is mainly non-strange [16]. In this analysis the following values have been used :

$$Br(B_s^0 \to D\mu X) = 10.8 \pm 0.4\%$$

$$Br(B_s^0 \to D_s\mu X) = (0.85 \pm 0.05) \times Br(B_s^0 \to D\mu X)$$

The main sources of background have been evaluated from the Monte Carlo simulation, which has been found to describe them correctly in the analysis of inclusive muon production [14] .
These are :

- events tagged by a non prompt or fake muon (the main sources are light hadron decays and hadronic punch-through)(figure 7-g). They amount to about 40 % of all the candidates. Their contribution is greater at low p_t^μ, while for p_t^μ greater than 1 GeV/c it amounts to 20 ± 7 % of the candidates. The contribution of this contamination has been evaluated from a Monte Carlo sample of size close to that of the data.
- events tagged by a prompt muon with the ϕ meson produced as part of the original b-quark fragmentation (figure 7-h). This contribution is expected to be small, about 5 %.
- events tagged by a prompt muon with the ϕ meson a decay product of the B meson and not a secondary charm particle. Contributions from non-strange B meson decays are expected to be negligible since these originate from Cabibbo suppressed transitions or non-planar hadronization mechanisms which require the presence of an $s\overline{s}$ quark pair (figure 7-i). In case of strange B hadron decays there could be a contribution from normal (planar) hadronization processes that require the presence of a $s\overline{s}$ quark pair. Monte Carlo simulation suggests that this source can also be neglected.

The one remaining parameter, f_s^w, has been determined by comparing the p_t^μ distribution to the sum of the distributions predicted from Monte Carlo simulation for the

various contributing processes. The relative contribution of each predicted distribution is set equal to the central values of the branching fractions quoted above. Minimizing the χ^2 over 4 p_t^μ bins, the probability of a b-quark fragmenting to a B_s^0 meson is determined to be

$$f_s^w = 0.18 \pm 0.12(stat).$$

The various contributions in the 4 p_t^μ bins are summarized in Table 2 and shown in figure 8.

Table 2: Number of $\phi - \mu$ events in data and in Monte Carlo simulation

$\phi - \mu$ candidates	p_t (0.0-0.4)	p_t (0.4-0.8)	p_t (0.8-1.2)	$p_t > 1.2$	Processes
DATA	12.0±7.0	11.0±7.7	11.3±6.3	16.7±5.7	
MC - non-prompt muons	7.3	7.3	4.4	2.9	
MC - direct charm	4.6	1.2	0.3	0.3	P_3^f
MC - cascade decays	2.1	6.3	0.9	0.4	$P_2^c + P_2^d + P_2^e$
MC - direct beauty	0.6	0.8	2.7	11.6	$P_1^a + P_1^b$

As shown in figure 8-a muons from direct B decays account for 80% of the candidates at transverse momenta larger than 1.2 GeV/c. In figure 8-b the fit to the data is shown and compared with the predictions obtained for $f_s^w = 0$ and $f_s^w = 0.40$.

The efficiency of the selection has been measured using a Monte Carlo sample equivalent to four times the data statistics and was found to be

$$\epsilon(direct\,beauty) = 10.0 \pm 0.9\%$$

$$\epsilon(cascade\,decay) = 5.0 \pm 0.9\%$$

$$\epsilon(direct\,charm) = 6.1 \pm 1.5\%$$

for the three classes of events. The differences in the acceptances for the different classes are mainly due to the minimum muon momentum (2.0 GeV/c) and ϕ meson energy requirements.

Differences between data and Monte Carlo generated events have been investigated, the main one being due to the requirement of at least 2 VD hits associated to the muon. The efficiency of the VD cuts used to select the $\phi - \mu$ candidates has been determined from the data, using the decay chain $D^{\star+} \to D^0\pi^+$ where the D^0 decays into $K^-\pi^+$. A $D^{\star+}$ signal of about 300 events is observed without any vertex detector requirement. The cuts used in selecting the $\phi - \mu$ candidates have then been applied to both data and Monte Carlo $D^{\star+}$ candidate events. Other minor differences come from the cut on the χ^2 of the secondary vertex fit and from the muon identification [14]. The efficiency determined from Monte Carlo was then corrected by the factor 0.78 ± 0.07 which takes into account all these effects.

The systematic uncertainty on the value of f_s^w has been obtained by varying the parameters inside their respective acceptable range of values. The results of this study are summarized in Table 3. The total absolute variation is 0.08. The partial correlation between the branching ratio of $D_s \to \phi\pi$ and of $D_s \to \phi\mu\nu$ has been taken into account [16] (see first row of table 3). The largest systematic uncertainty comes from poor knowledge of the decay branching fractions of the D_s meson. The contribution coming from all the other parameters not reported in Table 3 has been verified to be between 0.005 - 0.01.

The result is

$$f_s^w = 0.18 \pm 0.12(stat) \pm 0.08(syst).$$

Table 3: Systematic errors on f_s^w determination

Systematic Source	Range of variation	Absolute variation of f_s^w
$Br(D_s \to \phi\pi)$ $Br(D_s \to \phi\mu\nu)$ corr.	3.0 ± 0.7 % 1.5 ± 0.3 %	−0.06 + 0.04
$Br(D_s \to \phi\pi)$	3.0 ± 0.7 %	∓ 0.025
$Br(D_s \to \phi)$ X	(4.8 ± 0.5) Br($D_s \to \phi\pi$)	∓ 0.01
DATA/MC eff. corr. factor	78 ± 8 %	± 0.04
selection efficiency : • Hadron misidentified • Processes 1, 2, 3	 40 ± 8 % ± 20 %	 ∓ 0.03 ∓ 0.03

4.3 B_s^0 meson lifetime

In the preceding section it has been shown that the B signal to background ratio increases as the cut on the muon transverse momentum is increased. The B_s^0 lifetime measurement has, therefore, been restricted to events containing a muon with p_t^μ greater than 1 GeV/c. To increase the statistics, $\phi-electron$ events with p_t^{el} greater than 1 GeV/c have been included in the analysis. Above this p_t the purity of the identified electron sample is similar to that of the muon sample. The contamination from misidentified hadrons is at the level of 20 %. The combined ϕ signal contains 31 ± 8 events as shown in the inset of Fig. 9, which have to be compared with the 22 ± 6 events obtained with the muons alone (Fig. 6-b).

Using the values of ϕ meson production rate in D meson decays [13] and the probabilities for D^0, D^+, or ${D_s}^+$ meson production in B semileptonic decays [15], the purity of B_s^0 in the $\phi - l$ sample, from B decays, is determined to be

$$\frac{N_{evts}(B_s^0 \to \phi l X)}{N_{evts}(B \to \phi l X)} = 66 \pm 8(stat) \ {}^{+\ 13}_{-\ 16}(syst)\ \%$$

In the calculation of the decay time of the B meson, two physical quantities need to be determined : the flight distance and the energy of the B meson.

The K^+K^-l pseudo-vertex is a good estimator of the B decay vertex as it has been verified using the Monte Carlo simulation. The distance (d_{meas}) between the primary vertex and the K^+K^-l vertex has been compared with the generated B flight distance (d_{gen}) from a sample of $B_s^0 \to D_s \to \phi l X$ Monte Carlo generated events. The distribution of ($d_{meas} - d_{gen}$) has been found to have a mean value of 30 μm with a resolution of 330 μm indicating that the bias introduced in determining the lifetime using d_{meas} is negligible. This result comes from the small decay distance of the D_s meson from the B decay and the small opening angle between the K^+ and the K^- from the ϕ decay.

The energy of the B meson has been evaluated from the momentum of the $\phi - l$ system. A linear relation between the fraction of the B momentum carried by the $\phi - l$ system and the momentum of the $\phi - l$ system is observed in the Monte Carlo :

$$\frac{p(\phi l)}{p(B)} = a + b \times p(\phi l)$$

with $a = 0.215 \pm 0.014$ and $b = 0.018 \pm 0.005 \quad (GeV/c)^{-1}$.

Using this relationship the B momentum is determined with a mean resolution of 17 %. The resolution improves with increasing energy of the $\phi - l$ system. The proper decay time distribution obtained is shown in figure 9.

A maximum likelihood fit has been performed on the proper time distribution with the fitting function containing two terms, one describing the signal and the other the background, weighted according to their relative proportions. The proper-time distribution for the signal is obtained from an exponential convoluted with a Gaussian whose width is evaluated for each event, taking into account the accuracy on the actual vertex determination and the resolution on the B momentum. The proper-time distribution for the background has been obtained from events selected in the wings of the ϕ meson signal. It contains two components, one of zero lifetime, which accounts for about 50 % of the events, and one with a lifetime of 1.54 ps (arising essentially from semi-leptonic non-strange B decays). Their proper time distributions are convoluted with Gaussian distributions to account for the finite accuracy of the proper-time determination. The fraction (20 %) of the events which corresponds to genuine ϕ mesons associated to hadrons misidentified as leptons is assumed to have the same lifetime distribution as background events. This assumption is justified in the present situation of low statistics.

The lifetime of this sample is determined to be

$$\tau(B \to \phi l) = 1.18 \ {}^{+0.44}_{-0.36}(stat) \pm 0.15(syst) \ ps.$$

The systematic error is dominated by the uncertainty in the parametrisation of the background distribution and its lifetime. Using the value for the B_s^0 purity of 66 % $\pm$ $8(stat) \ {}^{+}_{-} \ {}^{13}_{16}(syst)$ % obtained above, and taking the measured average value for the B meson lifetime [12], the B_s^0 lifetime is found to be

$$\tau(B_s^0) = 1.08 \quad \pm 0.73 \, ps.$$

This result is consistent with the one recently published by OPAL [17].

5 Conclusions

From the measured production rates of D_s mesons and of $\phi - \mu$ events, the probability that a b quark combines with a strange antiquark to form a strange B_s^0-meson in the hadronization process has been measured to be

$$f_s^w = 0.24 \pm 0.08(stat)^{+0.15}_{-0.09}(syst)$$

and

$$f_s^w = 0.18 \pm 0.12(stat) \pm 0.08(syst)$$

respectively.

In both analyses the largest contributions to the systematic error come from poor knowledge of the D_s and B_s^0 branching fractions. From the measurement of the production rate of D_s-lepton in the same jet [1] f_s^w was determined to be

$$f_s^w = 0.17 \pm 0.08(stat) \pm 0.06(syst).$$

Combining these three measurements the following value has been obtained :

$$f_s^w = 0.19 \pm 0.06(stat) \pm 0.08(syst).$$

From the decay time distributions, the lifetimes for the D_s and $\phi - lepton$ samples have been measured to be

$$\tau(B \to D_s X) = 0.94\ ^{+0.35}_{-0.24}(stat) \pm 0.15(syst)\ ps$$

$$\tau(B \to \phi l\nu X) = 1.18\ ^{+0.44}_{-0.36}(stat) \pm 0.15(syst)\ ps$$

Taking into account the purities of B_s^0 in these two samples and combining them with a previous result obtained by this collaboration with $D_s - \mu$ events [1],

$$\tau(B \to D_s l\nu X)/\tau(B) = 0.8 \pm 0.4,$$

the B_s^0 meson lifetime is measured to be

$$\tau(B_s^0) = 0.96 \pm 0.37\ ps.$$

Acknowledgements

We are greatly indebted to our technical collaborators and to the funding agencies for their support in building and operating the DELPHI detector, and to the members of the CERN-SL Division for the excellent performance of the LEP collider.

References

[1] P. Abreu et al. (DELPHI Collaboration), Phys. Lett. B289 (1992) 199;
see also: D. Buskulic et al. (ALEPH Collaboration), Phys. Lett. B294 (1992) 145;
P.D. Acton et al. (OPAL Collaboration), Phys. Lett. B295 (1992) 357.

[2] P. Aarnio et al. (DELPHI Collaboration), " The DELPHI Detector ", Nucl.Instr. and Meth. A303(1991) 233-276.

[3] N. Bingefors et al. (DELPHI Collaboration), "The DELPHI Microvertex Detector", to be published in Nucl. Instr. and Meth.

[4] T. Sjöstrand, Comp. Phys. Comm. 27 (1982) 243, ibid. 28 (1983) 229.
T. Sjöstrand and M. Bengtsson, Comp. Phys. Commun. 43 (1987) 367.

[5] M. Suzuki, Phys. Rev. D 31 (1985) 1158.

[6] D.G. Cassel, in Physics in Collision 10, eds. A. Goshaw and L. Montanet, (Editions Frontieres, Dreux, 1990) p. 276.

[7] P. Abreu et al. (DELPHI Collaboration), Z. Phys. C57 (1993) 181.

[8] H. Albrecht et al. (ARGUS Collaboration), Z. Phys. C54 (1992) 1.

[9] D. Bortoletto et al. (CLEO Collaboration), Phys. Rev. D 37 (1988) 1719.

[10] D. Bortoletto et al. (CLEO Collaboration), Phys. Rev. Lett. 64 (1990) 2117.
H. Albrecht et al. (ARGUS Collaboration), Z. Phys. C54 (1992) 1.

[11] M. Zito, Ph.D. Thesis University Paris XI Orsay, DAPNIA/SPP 93-12 (1993).

[12] P.S. Drell and J.R. Patterson, in Proc. of the XXVI Int. Conf. on High Energy Physics, J. Sanford ed., Dallas (1992), vol. 1 pag. 3.

[13] P. Roudeau and A. Stocchi " Inclusive branching fractions of D^0 , D^+ and D_s into ϕ mesons " LAL 93-03 (1993).

[14] P. Abreu et al. (DELPHI Collaboration), Z. Phys. C56 (1992) 47.

[15] K. Berkelman and S.L. Stone, Ann. Rev. of Nuclear and Particle Science V41 (1991) 1.

[16] A. Stocchi, Ph.D. Thesis, University Paris XI Orsay, LAL 93-10 (1993).

[17] P.D. Acton et al. (OPAL Collaboration), Phys. Lett. B312 (1993) 425.

6 Figure Captions

- Fig. 1 : Quark diagrams contributing to inclusive D_s meson production.
- Fig. 2 : K^+K^- mass distribution for particles with momentum greater than 2 GeV/c and measured ionization in the TPC consistent with that of a kaon. The curve shows the result of a fit with a Gaussian and a term for the background. The latter has been parametrized with the function $B(m) = p_1 m^{p_2}(1 + p_3 m + p_4 m^2)$, where $m = m(KK) - 2m_K$.
- Fig. 3 : Invariant mass distribution of the $\phi\pi$ candidates. The curve shows the result of a fit with a Gaussian and a term for the background. The latter has been parametrized with the exponential of a second order polynomial.
- Fig. 4 :
  - 4-a) $|cos(\psi)|$ distribution for the events selected in the D_s signal region after combinatorial background subtraction.
  - 4-b) Transverse momentum distribution of the selected D_s candidates. The Monte Carlo predictions for D_s meson production for $b\overline{b}$ and $c\overline{c}$ events are shown as dotted and hatched histograms respectively.
- Fig. 5 : The measured B proper time distribution for the D_s sample, shown by the points with the error bars. The curve is the result of the likelihood fit. The shaded area corresponds to the background distribution. In the inset is plotted the invariant mass distribution of the $\phi\pi$ candidates used for the lifetime measurement after tighter selection cuts.
- Fig. 6 : ϕ meson signal in events accompanied by a muon in the same jet: a) with no muon transverse momentum cut, and b) with a muon transverse momentum greater than 1 GeV/c. The curves are the result of the fit of the mass spectrum using a Gaussian distribution for the signal and the same parametrization for the background as in fig. 2.
- Fig. 7 : Processes contributing to the production of $\phi - \mu$ events with the ϕ and the muon appearing in the same jet. When several mechanisms of the same type contribute to a given process, only the dominant diagram has been displayed.
- Fig. 8 : Transverse momentum distribution of the muon in $\phi - \mu$ events. The last bin contains all events with p_t^μ greater than 1.2 GeV/c.
  - a) Data (points with error bars) and contributions from (i) fake muons (cross-hatched), (ii) direct muons from D mesons (dense cross-hatched), (iii) cascade muons (diagonal hatched) and (iv) direct muons from B_s^0 mesons (dark-hatched).
  - b) Data compared with expectations for different values of f_s^w: (i) 0.2 (the fit result - dashed), (ii) 0.0 (dotted), and (iii) 0.4 (dash-dotted)
- Fig. 9 : Measured proper time distribution of $\phi - l$ events. The curve is the result of the likelihood fit. The shaded area corresponds to the background distribution. In the inset is plotted the invariant mass distribution of the ϕ candidates used for the lifetime measurement. The curve is the result of the fit of the mass spectrum using a Gaussian distribution for the signal and the same parametrization for the background as in fig. 2.

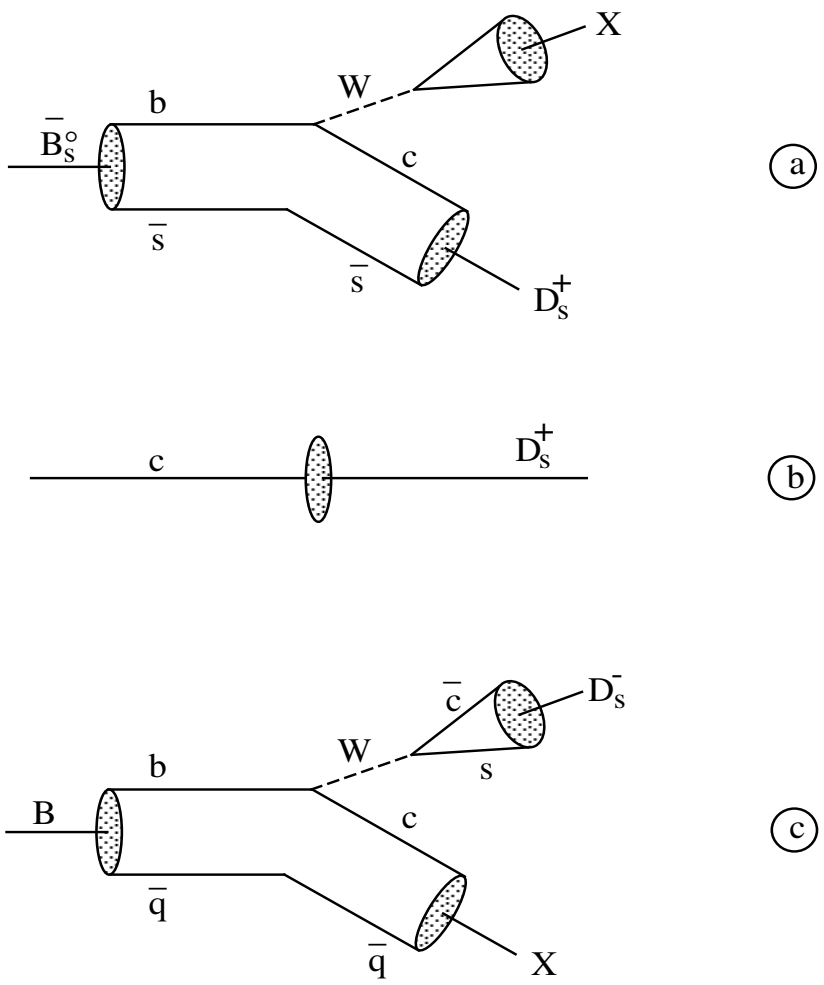

Fig. 1

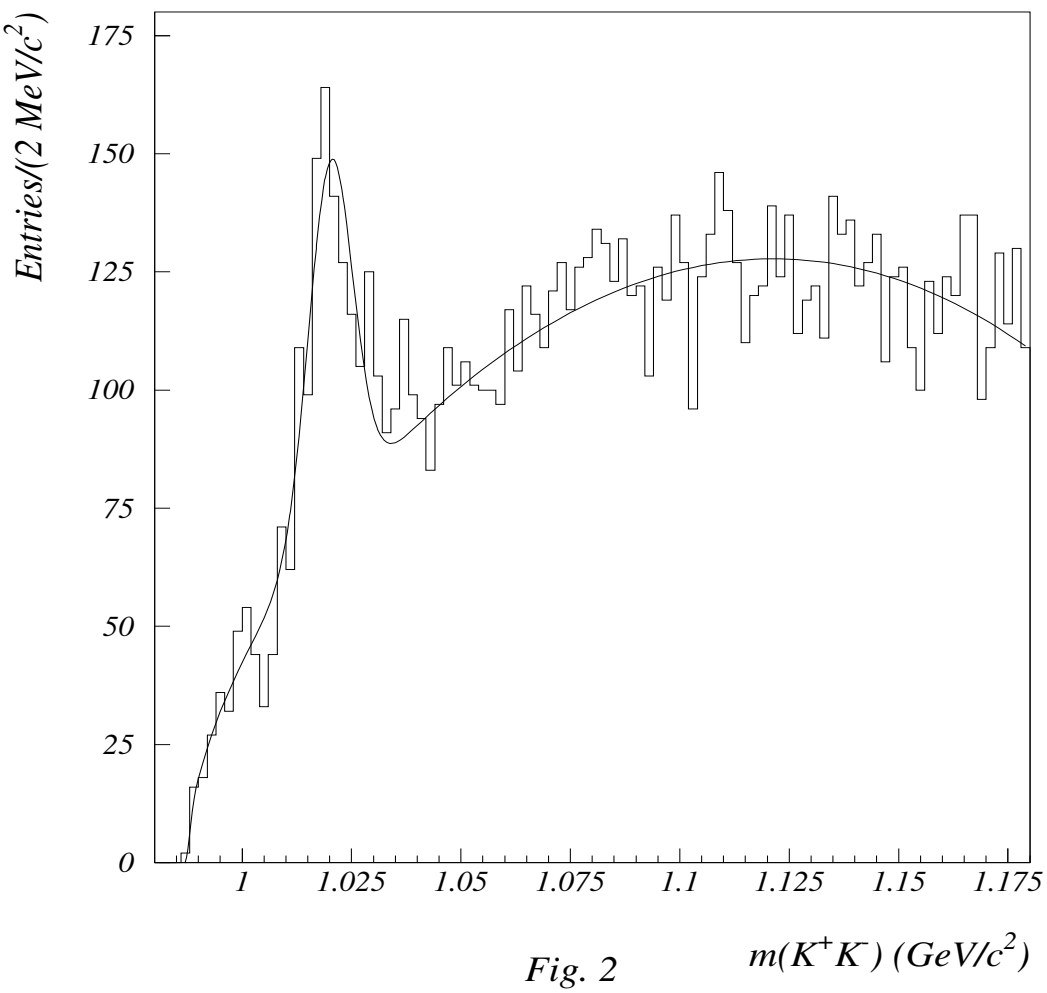
Entries/(2 MeV/c²)
175
150
125
100
75
50
25
0
1
1.025
1.05
1.075
1.1
1.125
1.15
1.175
m(K⁺K⁻) (GeV/c²)

Fig. 2

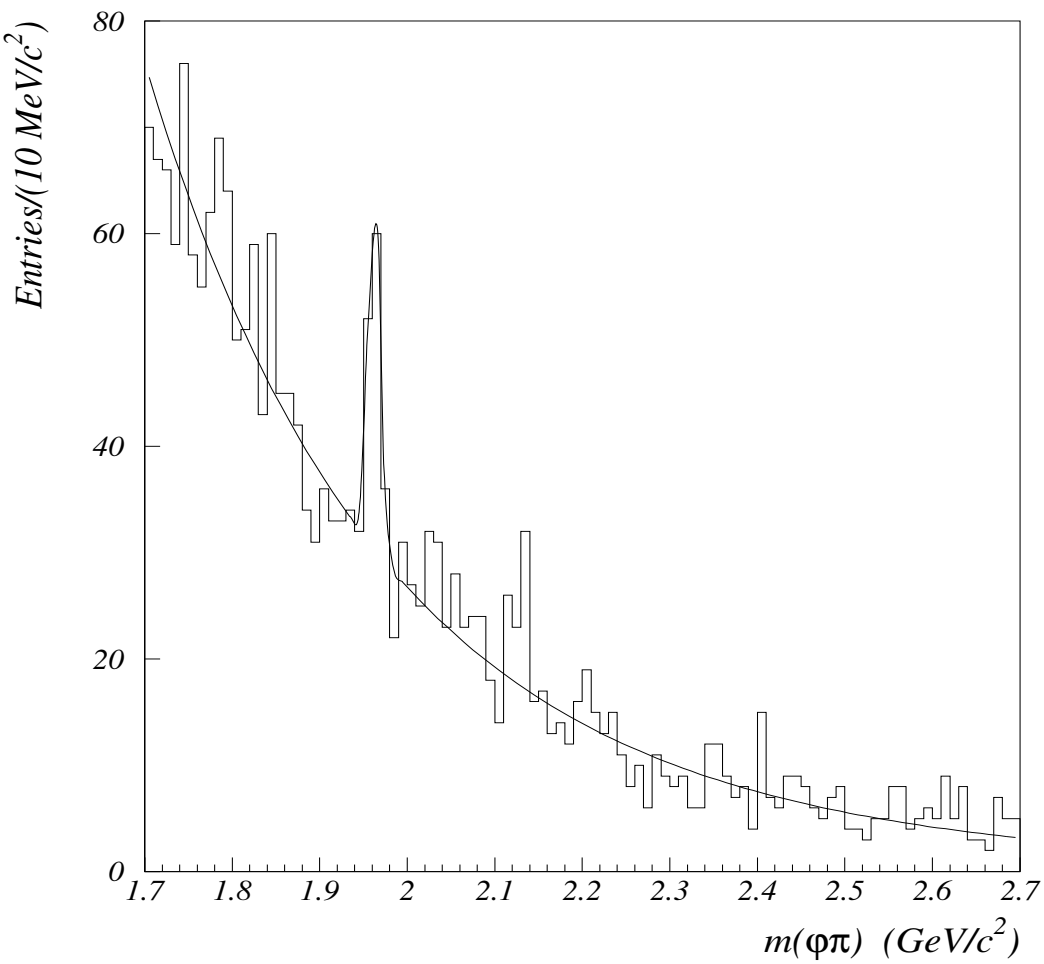
Entries/(10 MeV/c²)
80
60
40
20
0
1.7
1.8
1.9
2
2.1
2.2
2.3
2.4
2.5
2.6
2.7
m(φπ) (GeV/c²)

Fig. 3

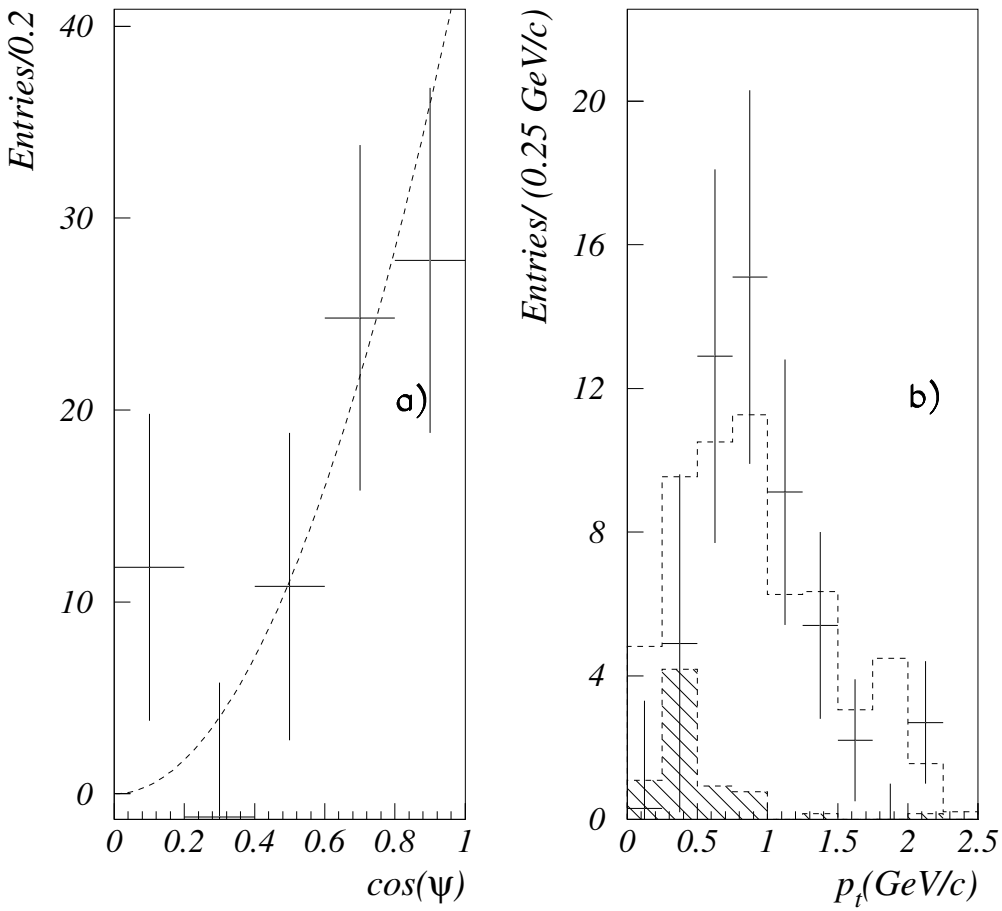
Entries/0.2
40
30
20
10
0
0
0.2
0.4
0.6
0.8
1
cos(ψ)
a)
Entries/ (0.25 GeV/c)
20
16
12
8
4
0
0
0.5
1
1.5
2
2.5
p_t(GeV/c)
b)

Fig. 4

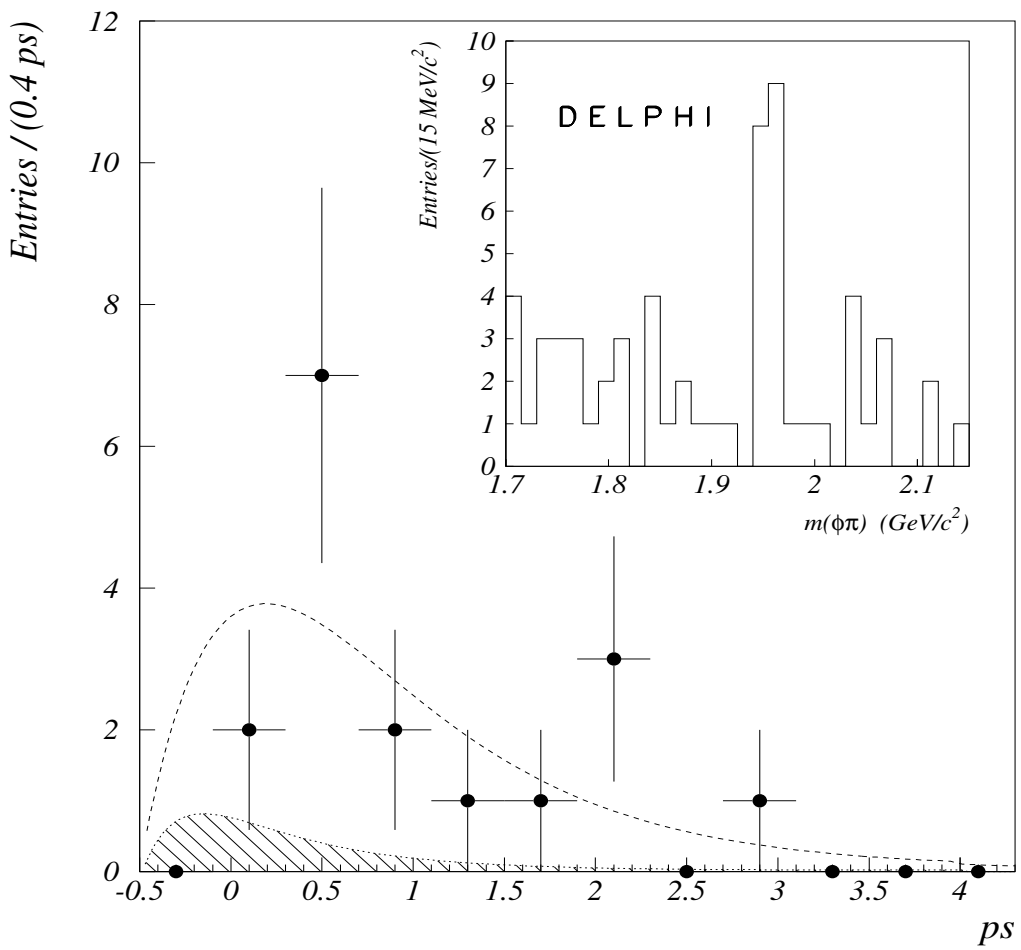

Fig. 5

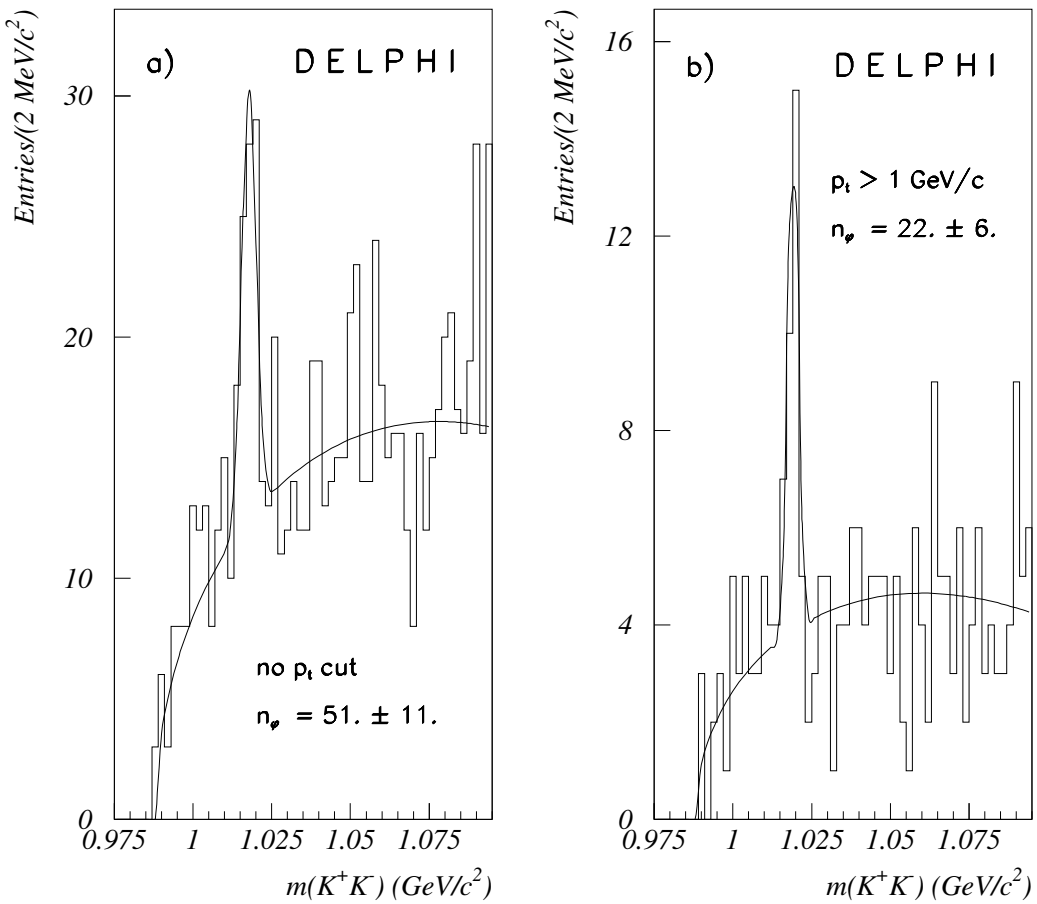
a)
DELPHI
no p_t cut
n_φ = 51. ± 11.
Entries/(2 MeV/c^2)
$m(K^+K^-)$ (GeV/c^2)
b)
DELPHI
p_t > 1 GeV/c
n_φ = 22. ± 6.
Entries/(2 MeV/c^2)
$m(K^+K^-)$ (GeV/c^2)

Fig. 6

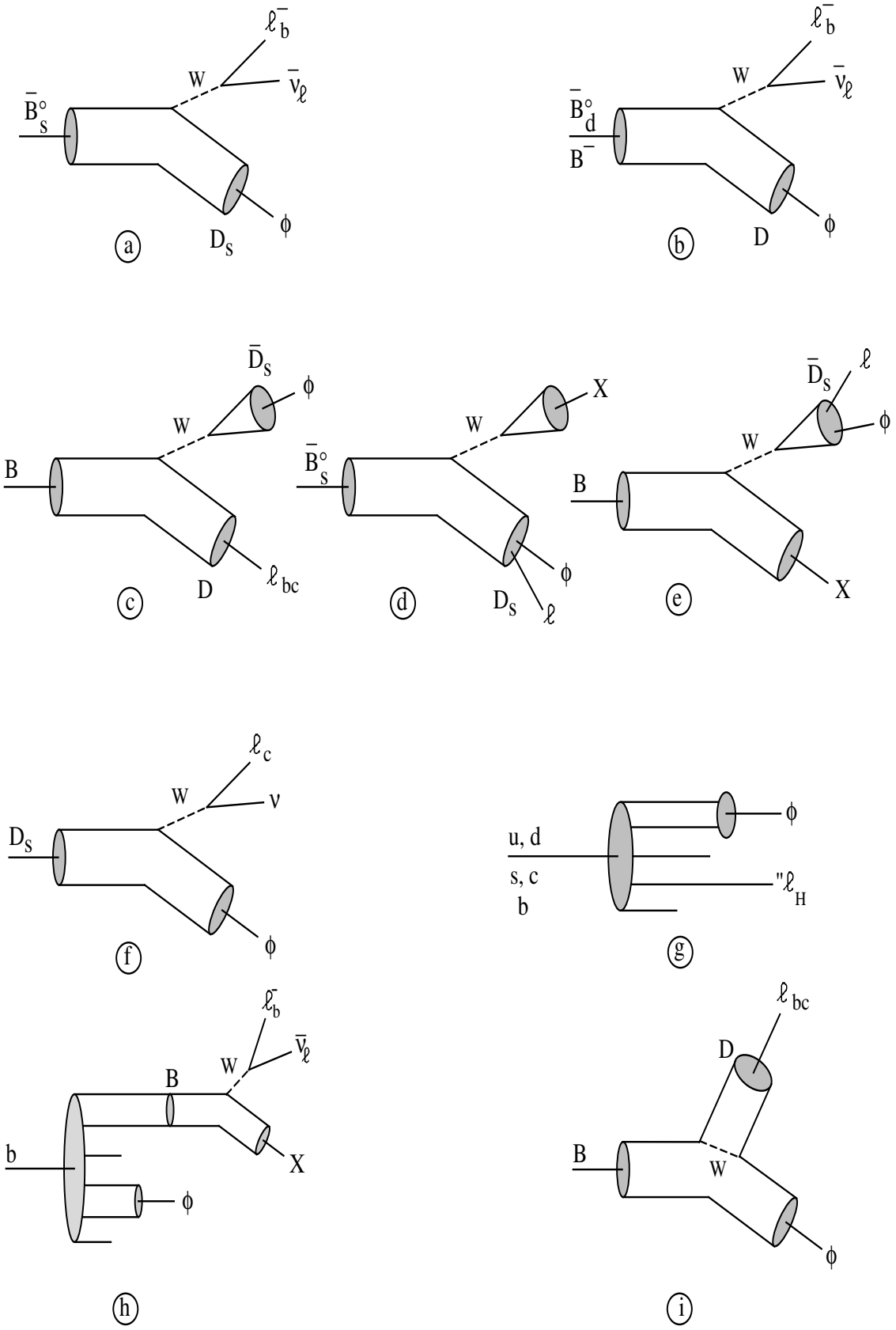
$\bar{B}_s^\circ$
W
ℓ_b^-
$\bar{\nu}_\ell$
D_S
ϕ
a
$\bar{B}_d^\circ$
B^-
D
b
B
$\bar{D}_S$
ℓ_{bc}
c
$\bar{B}_s^\circ$
X
d
ℓ
e
u, d
s, c
b
"ℓ_H
f
g
h
i

Fig. 7

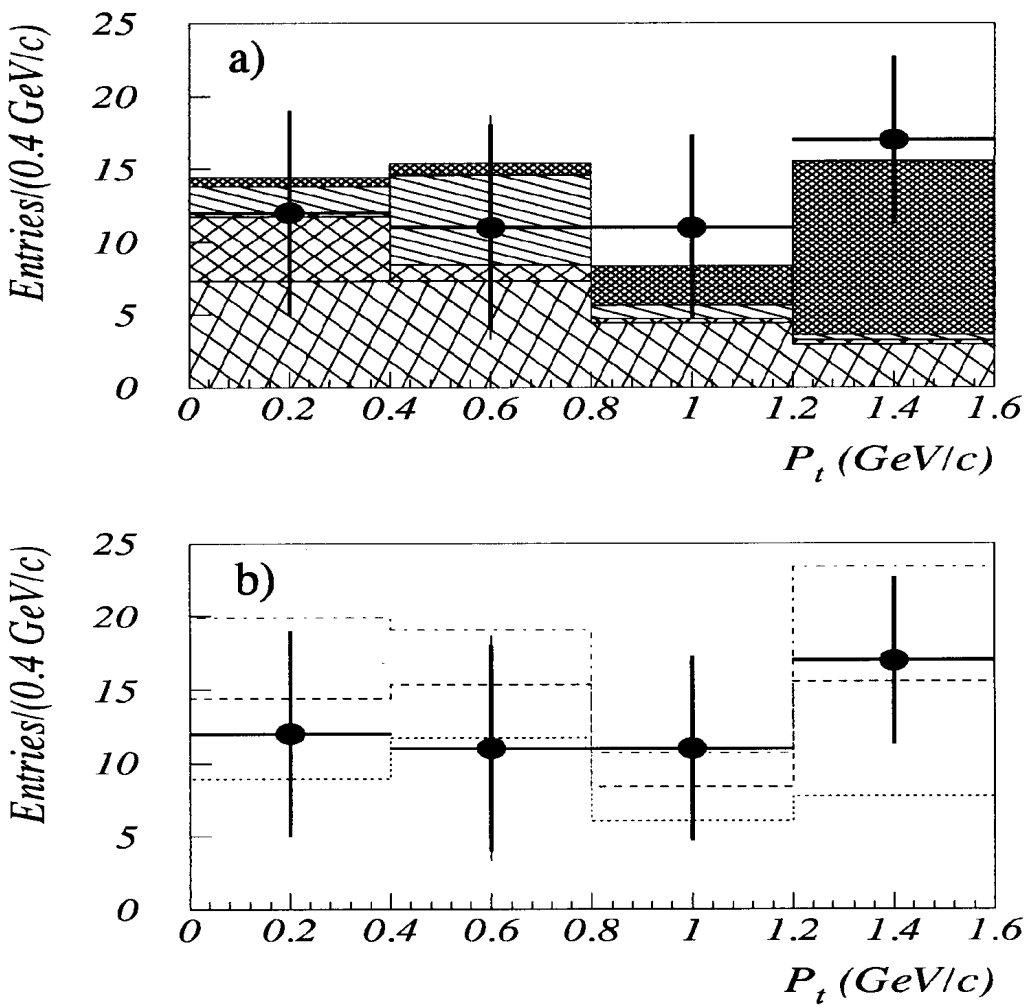

Fig. 8

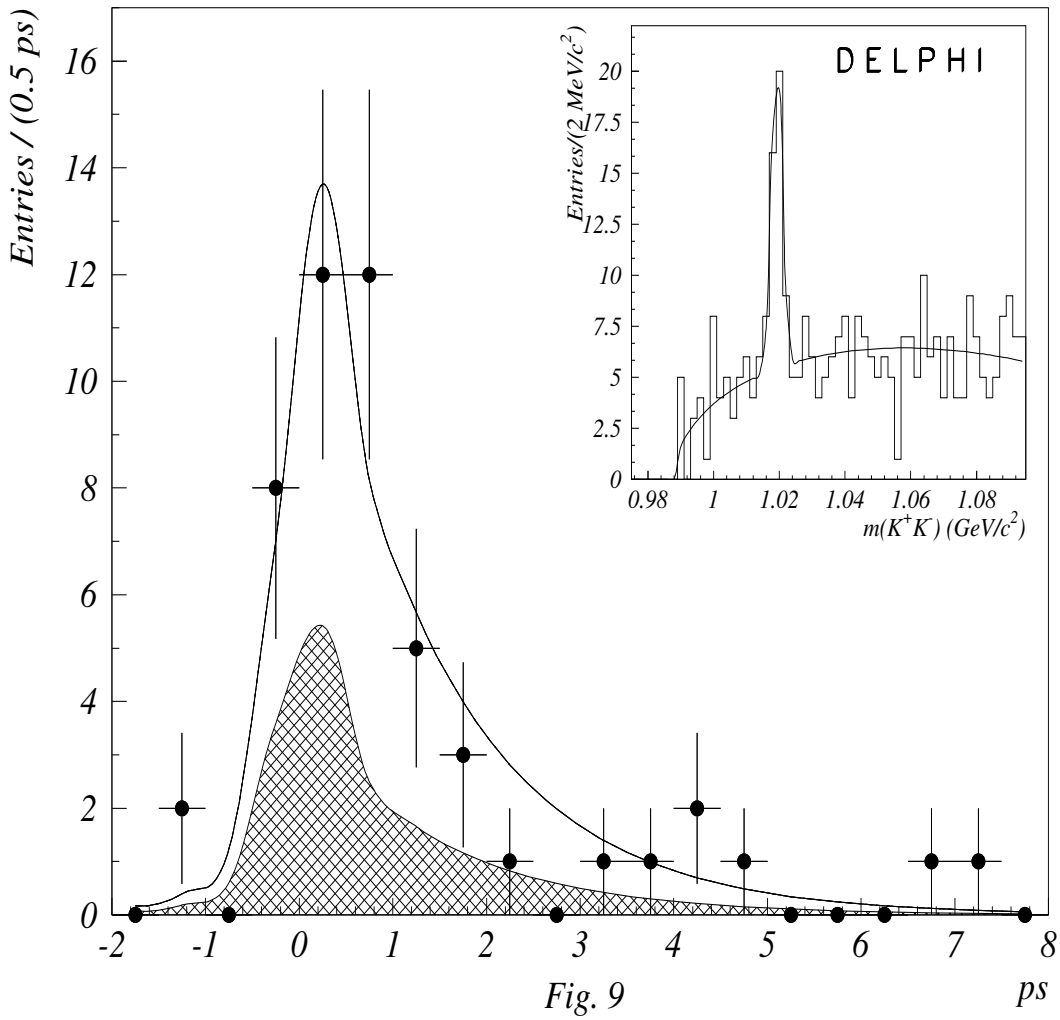

Fig. 9